Effect of the Germanium Incorporation in the Synthesis of EU-1, ITQ-13, ITQ-22, and ITQ-24 Zeolites

German Sastre, Angeles Pulido, Rafael Castañeda, and Avelino Corma*

Instituto de Tecnologia Quimica. UPV−CSIC, Av/Los Naranjos s/n, 46022 Valencia, Spain

Received: December 12, 2003; In Final Form: April 20, 2004

Computational chemistry is used here to rationalize zeolite nucleation and crystallization by means of atomistic molecular mechanic techniques. It is shown that, by isomorphous substitution of Ge by Si, the relative rate of crystallization can be reversed in a series of zeolite structures that compete to nucleate and grow under certain synthesis conditions. This is demonstrated for EU-1, ITQ-13, ITQ-22, and ITQ-24 structures.

1. Introduction

Organic structure directing agents (SDAs) are commonly used in the synthesis of zeolites to achieve the crystallization of new structures.[1,2] SDAs are important in the nucleation and growth of zeolites, but very seldom do they act as real templates of a particular structure.[3] Indeed, other synthesis variables, such as temperature, water/silica ratio, the presence (or absence) of alkaline cations, the silica mobilizing anion (OH^- or F^-), and the nature of framework cations (such as Ge, among others), can be determinant for the particular structure obtained.[4−11] It is then not surprising that, using the same SDA but different alkaline cations (Na^+, K^+), two different structures—SSZ-31 and SSZ-24—have been obtained.[12] Also, with *N*-benzylquinuclidine, either β or SSZ-42 are crystallized when the framework T^{III} cation is either Al or B.[13] Unfortunately, it becomes difficult in most cases to explain the determinant role that variables other than the SDA can play to direct into several close structures. In a very interesting paper, Harris and Zones[14] showed the nature of the interactions between the zeolite microcavity and the SDA, and they related the strength of this interaction, mostly of van der Waals type, with the crystallization time of nonasil and SSZ-13 zeolites.

In the present study, we have used hexamethonium as the SDA, which, under the experimental conditions tested, is able to produce EU-1, ITQ-13, ITQ-22, and ITQ-24 zeolites. We study first the pure silica structures and then the effect of germanium and fluorine incorporation, and then how the selectivity of the synthesis is influenced by the short- and long-range interactions of the SDA with the zeolite structure. Moreover, and using the same theoretical methodology, we show that the relative rate of crystallization can be practically reversed when the silica mobilizing agent and the zeolite framework composition is changed. The theoretical results closely match those of the preferred zeolite that has been synthesized and their stability has been measured experimentally.

2. Experimental Section

2.1. Preparation of Hexametilen-bis(trimethylammonium) Dibromide. A quantity of 37.38 g of 1,6-dibromohexane (96% purity, Aldrich), plus 82.35 g of trimethylamine solution (31−35 wt % in ethanol), and ethanol in the approximate proportion to provide a good mixture, were added to a 500 mL flask, and mixed with a magnetic stirrer for 2 days at ambient temperature. The mixture then was directly washed with ethyl acetate and diethyl ether and the product, hexamethonium dibromide, was recovered using the gravity filtration technique. Afterward, the white solid obtained was left to dry for 12 h at ambient temperature and then stored.

2.2. Preparation of Hexamethonium Dihydroxide. Hexamethonium dihydroxide was prepared by direct anionic exchange using a resin, Amberlite IRN-78 (Supelco), as the hydroxide source; the resin was washed with Milli-Q water (Millipore) prior to its use until the water pH was 7. The procedure involved the dissolution of 9 g of hexamethonium dibromide in 250 g of Milli-Q water. The resulting solution was placed into contact with the prior-washed resin into an exchange column, and the flow rate was regulated to obtain an exchange yield of >95%. The solution of hexamethonium dihydroxide was collected into a beaker. This solution was concentrated at 50 °C and kept under vacuum until the hydroxide concentration was >0.05 mol/kg.

2.3. Synthesis of the Boron-Containing ITQ-24 Material. GeO_2 (1.437 g) and 0.204 g of boric acid were dissolved in 161 g of a hexamethonium dihydroxide solution (concentration of 0.256 mol/kg). A quantity (14.311 g) of tetraethylorthosilicate (TEOS) was added to the resulting solution, and the mixture was mechanically stirred at 200 rpm, until the hydrolysis of TEOS had been completed and the ethanol generated was totally evaporated. The final synthesis gel had the following molar composition:

$$5SiO_2{:}1GeO_2{:}1.50R(OH)_2{:}30H_2O{:}0.12B_2O_3$$

where $R(OH)_2$ is hexamethonium dihydroxide.

The gel was autoclaved at 175 °C for 15 days under continuous stirring at 60 rpm, and the solid was recovered by filtration, washed with distilled water, and dried at 100 °C overnight.

2.4. Synthesis of the ITQ-22 Material. GeO_2 (0.7185 g) were dissolved in 80.5 g of a hexamethonium dihydroxide solution (concentration of 0.256 mol/kg). TEOS (7.156 g) was added to the resulting solution, and the mixture was mechanically stirred at 200 rpm, until the hydrolysis of TEOS had been completed and the ethanol generated was totally evaporated. The final synthesis gel had the following molar composition:

$$5SiO_2{:}1GeO_2{:}1.50R(OH)_2{:}30H_2O$$

where, again, $R(OH)_2$ is hexamethonium dihydroxide.

The gel was autoclaved at 175 °C for 15 days under continuous stirring at 60 rpm, and the solid was recovered by filtration, washed with distilled water, and dried at 100 °C overnight.

* Author to whom correspondence should be addressed. E-mail address: acorma@itq.upv.es.

10.1021/jp0378438 CCC: $27.50
Published on Web 05/27/2004

2.5. Synthesis of the ITQ-13 Material. GeO_2 (0.785 g) was dissolved in 161 g of a hexamethonium dihydroxide solution (concentration of 0.256 mol/kg). TEOS (15.621 g) was added to the resulting solution, and the mixture was mechanically stirred at 200 rpm, until the hydrolysis of TEOS had been completed and the ethanol generated was totally evaporated. The final synthesis gel had the following molar composition:

$$10SiO_2{:}1GeO_2{:}2.75R(OH)_2{:}55H_2O$$

where, again, $R(OH)_2$ is hexamethonium dihydroxide.

The gel was autoclaved at 175 °C for 25 days under continuous stirring at 60 rpm, and the solid was recovered by filtration, washed with distilled water, and dried at 100 °C overnight.

2.6. Synthesis of the EU-1 Material. GeO_2 (0.785 g) was dissolved in 161 g of a hexamethonium dihydroxide solution (concentration of 0.256 mol/kg). TEOS (15.621 g) was added to the resulting solution, and the mixture was mechanically stirred at 200 rpm, until the hydrolysis of TEOS had been completed and the ethanol generated was totally evaporated. The final synthesis gel had the following molar composition:

$$10SiO_2{:}1GeO_2{:}2.75R(OH)_2{:}110H_2O$$

where, again, $R(OH)_2$ is hexamethonium dihydroxide.

The gel was autoclaved at 175 °C for 25 days under continuous stirring at 60 rpm, and the solid was recovered by filtration, washed with distilled water, and dried at 100 °C overnight.

2.7. Calcination of the Materials. The occluded hexamethonium was removed from the samples by heating the products from room temperature to 300 °C at a rate of 1 °C/min, and that latter temperature was maintained for 3 h. The next step involved increasing the temperature at a rate of 1 °C/min up to 580 °C; the product was kept at this temperature for 3 h, to burn off the remaining organic material.

All the samples (ITQ-22, ITQ-24, ITQ-13 and EU-1) retained their structure after the calcination.

Germanium incorporation in the crystallized phase was always 100%, as measured by chemical analysis, and the concentration of SDA was, in all cases, 0.25 molecules/TO_2.

3. Theory

The computational results obtained take into account that the stabilization of the "zeolite−SDA" system, with respect to the separate components, is due to several energetic interactions between the guest and the zeolite as follows:

$$E_{\text{Total}} = E_{\text{zeo}'} + E_{\text{zeo}'-\text{SDA}} + \Delta E_{\text{SDA}} \quad (1)$$

3.1. $E_{\text{zeo}'}$. The first term, $E_{\text{zeo}'}$, refers to the stability of the final zeolite formed, which is formed with the SDA occluded. More-stable structures will have less energy and, therefore, will be favored. Note that we have used the subscript "zeo′" to indicate that the final optimized structure differs from an optimization without SDA occluded. Therefore, the flexibility of the structure and not just its intrinsic stability will contribute to this term, although it is expected that the latter will be the most important contribution.

3.2. $E_{\text{zeo}'-\text{SDA}}$. The contribution $E_{\text{zeo}'-\text{SDA}}$ corresponds to the interactions between the zeolite structure and the organic SDA. This term is more favorable when an adequate match between the SDA shape and the micropore is observed. Although not in all cases, the most important contribution to this will be the short-range interactions, which account mainly for the electronic interactions between the organic and the zeolite walls. Nevertheless, charged SDAs will direct trivalent heteroatoms near the positively charged region of the SDA. Although the latter is also part of this energetic term, here, we are only interested in the short-range contribution, which tells us about the selectivity of a zeolite structure formation with a given SDA. For this reason, SDAs included in the micropore volume will be considered with a charge distribution of zero total charge and zeolites will be considered pure silica composition, as in previous studies.[15] The role of the aluminum, which is also important, will be considered by calculating the maximum aluminum content of each structure, which, in turn, is dependent on the SDA loading that the structure can host, such that the zeolite and the SDA molecules give an electrically neutral system.

3.3. ΔE_{SDA}. The other term is ΔE_{SDA}, which accounts for the SDA deformation as occluded in the final zeolite micropore. Although this term is of an energetic nature, as are the others, some considerations that were made in a previous publication[15] lead us to relate this term with kinetic factors that are also of interest in considering the global synthesis process. Our rationalization was as follows: during the early stages of the nucleation, SDA molecules in conformations whose energy is achievable by thermal factors at the synthesis temperatures, are occluded by the silico-alumina oligomers that cluster around it, forming incipient cagelike units. The synthesis then progresses until the final structure is formed, and there, SDA molecules get occluded in those conformations, which do not necessarily correspond to the absolute minimum energy; we call these *high-energy conformations*. The SDA high-energy conformations are representative of the transition state of the reaction, and, in this sense, high ΔE_{SDA} values are indicative of processes that are not kinetically favored.[15]

4. Computational Methods

The calculations have been performed using lattice energy minimization techniques and the GULP code.[16] The interatomic potentials used to model the interactions between the atoms in the structure included the following terms: Coulombic interaction, short-range pair potentials (described by a Buckingham function), and a three-body bond bending term. The shell model was used to simulate the polarizability of the O atoms. A cutoff distance of 12 Å was applied to the short-range interactions (Buckingham- and Lennard-Jones-type interactions; see eqs 3 and 4 below). The Ewald summation technique has been used for the summation of the long-range Coulombic interactions. The potentials used for the zeolite[17,18] were parametrized to reproduce the structure of the α-quartz and have been demonstrated to model several zeotype structures successfully.[19−22] The force field by Kiselev et al.[23] was selected for the intermolecular SDA−zeolite and SDA−SDA interactions, the force field by Oie et al.[24] was selected for intramolecular interactions between the atoms of the SDA, and the force field by George and Catlow[25] was used for the F^- anions. More details on the computational methods can be found elsewhere.[26,27] The total potential energy function and the respective terms are as follows:

$$E_{\text{zeo}'} = E_{\text{Buckingham}} + E_{\text{Coulombic}} + E_{\text{three-body}} + E_{\text{core-shell}} \quad (2)$$

$$E_{\text{SDA}} = E_{\text{two-body}} + E_{\text{three-body}} + E_{\text{four-body}} + E_{\text{Coulombic}} \quad (3)$$

$$E_{\text{zeo}'-\text{SDA}} = E_{\text{Lennard-Jones}} \quad (4)$$

TABLE 1: Synthesis Results at 175 °C and under Different Experimental Conditions as Specified[a]

entry	Si/Ge ratio	water/Si ratio	[F⁻]	Si/Al ratio	phase(s)	time (days)
1	10	2.5	*b*	n.a.[c]	ITQ-22 + EU-1	30
2	10	5	*b*	n.a.[c]	ITQ-13	19
3	10	5	0.071	n.a.[c]	ITQ-22 + EU-1	19
4	10	7	0.56	n.a.[c]	ITQ-13	10
5	10	10	0.071	n.a.[c]	ITQ-13	15
6	10	10	*b*	50	EU-1	6
7	10	5	*b*	20	ITQ-24 + EU-1	17
8	5	2.5	*b*	n.a.[c]	ITQ-22	
9	5	5	*b*	n.a.[c]	ITQ-22	10
10	5	7	0.56	n.a.[c]	ITQ-13	7
11	5	10	*b*	n.a.[c]	EU-1	
12	5	5	*b*	40	ITQ-22 + ITQ-24	10
13	5	5	*b*	30	ITQ-24	
14	5	5	*b*	20	ITQ-24	10
15	5	5	*b*	10	amorphous	23

[a] Without germanium in the synthesis gel, laminar and amorphous compounds were obtained. Concentrations are given in molar composition, and a constant molar concentration ratio of $SDA/TO_2 = 0.25$ is observed in all cases. [b] No fluorine is present in the synthesis gel. [c] n.a. is a Si/Ge structure (without Al_2O_3 in the synthesis gel).

TABLE 2: Energetic Contributions and Total Energy (as from eq 1) to the Synthesis of EU-1, ITQ-13, ITQ-22, and ITQ-24 When Hexamethonium Dihydroxide is Used as a Structure Directing Agent (SDA)[a]

zeolite	$E_{zeo'}$ (eV/SiO_2)[b]	ΔE_{SDA} (eV)[c]	$\Delta E_{zeo'-SDA}$ (eV/SiO_2)[d]	ΔE_{Total} (eV/SiO_2)	[SDA][e]	Si/Al[f]
EU-1	−128.58	0.056	−0.056	−128.63	0.036	13.0
ITQ-13	−128.58	0.020	−0.056	−128.63	0.036	13.0
ITQ-22	−128.56	0.031	−0.053	−128.61	0.036	13.0
ITQ-24	−128.54	0.039	−0.066	−128.61	0.048	9.5

[a] These calculations correspond to pure silica zeolites with no F^- anions. [b] Framework energy of unloaded zeolites per SiO_2 unit (first term in eq 1). This corresponds to the zeolite geometry as with the SDA optimized inside. The corresponding number of SiO_2 units are 112 for EU-1, ITQ-22, and ITQ-24, and 56 for ITQ-13. The energies of the SiO_2 zeolites minimized without template are −128.582, −128.576, −128.561, and −128.544 eV/SiO_2 for EU-1, ITQ-13, ITQ-22, and ITQ-24 respectively. The densities for EU-1, ITQ-13, ITQ-22, and ITQ-24 are 1.79, 1.77, 1.67, and 1.59 g/cm^3, respectively. [c] Difference between SDA energy as optimized in the zeolite and in the ground state. This energy is the mean value between all the SDA molecules in the unit cell. The third term in eq 1 is calculated by averaging that energy difference to the number of SiO_2 units, rather than to the number of SDA molecules. [d] Stabilization energy due to the attractive short-range energy between the zeolite and the SDAs, per SiO_2 unit. This corresponds to the second term in eq 1. [e] Number of SDA molecules per SiO_2. [f] The Si/Al ratio corresponds to the maximum aluminum content when the micropores are filled with SDA. This is also shown in Table 4.

5. Results and Discussion

The experimental results (Table 1) show the synthesis products at 175 °C using hexamethonium dihydroxide, $[Me_3N-(CH_2)_6-NMe_3](OH)_2$ as SDA, in the synthesis gel. Table 2 shows the results of the simulations on EU-1, ITQ-13, ITQ-22, and ITQ-24, whose structures (with hexamethonium as optimized) are shown in Figures 1−4.

5.1. Role of the Hexamethonium. Table 2 shows that the total energy is lower for the EU-1 and ITQ-13 structures (−128.63 eV/SiO_2) and that these are the structures obtained experimentally at the higher Si/Ge ratio (Si/Ge = 10; see entries 5 and 6 in Table 1). The energetic contributions also show that this result is driven by the structural contribution, as indicated by the value −128.58 eV/SiO_2 for both EU-1 and ITQ-13 (Table 2), which is lower than that for ITQ-22 (−128.56 eV/SiO_2) and ITQ-24 (−128.54 eV/SiO_2) (see Table 2). Therefore, the structural factors ($E_{zeo'}$) rather than the factors related to the organic SDA ($E_{zeo'-SDA}$ and ΔE_{SDA}) seem to be driving the synthesis products. In a previous work, we studied the directing role of cyclohexyl alkyl pyrrolidinium salts in the synthesis of EU-1 and other structures, and values of −0.072 and −0.061 eV/TO_2 for $E_{zeo'-SDA}$ were determined for the methyl- and butyl-substituted organics, respectively,[15] whereas a value of −0.056 eV/TO_2 is found for hexamethonium in EU-1 (see Table 2), which shows that a better match in EU-1 is found for the pyrrolidinium salts than for the hexamethonium.

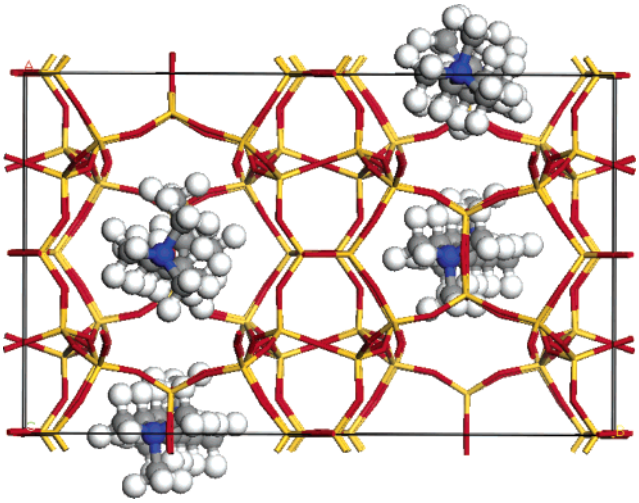

Figure 1. Structure of EU-1 with SDA (hexamethonium).

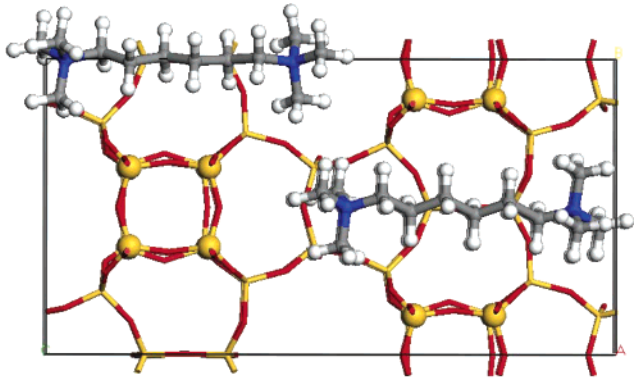

Figure 2. Structure of ITQ-13 with hexamethonium. T sites in D4R are highlighted.

More on the hexamethonium role can be obtained when the interaction energy of each individual hexamethonium cation with each microporous environment is calculated (Table 3). First, it can be seen that this energy is less favorable for large channel systems, formed by 12 MR (membered ring), similar to those of ITQ-22 and ITQ-24, for which energies of −1.38 and −1.23 eV are found, respectively. Also, the interaction energy is lowest (most favorable) for the smaller (10 MR) channels present in ITQ-22 and ITQ-24, which give energies of −1.58 and −1.60 eV, respectively. Channels with smaller diameter provide a shorter distance between the SDA and the zeolite atoms, thus making the interaction more favorable and further reducing the interaction energy. Intermediate energy values (between those of 10 MR and 12 MR) are observed for the cavities present in EU-1 and ITQ-13, where energies of −1.58 and −1.55 eV are obtained, respectively. Cavities with 12 MR sections are favored, with respect to 12 MR channels, because the cavities provide

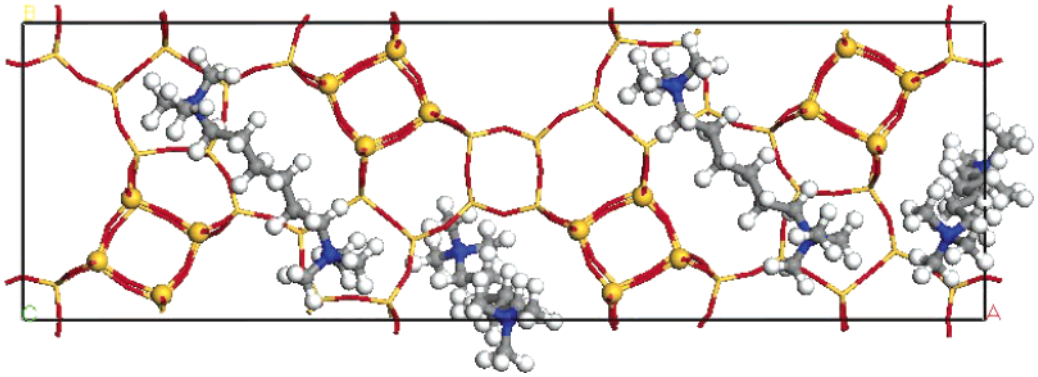

Figure 3. Structure of ITQ-22 with hexamethonium. T sites in D4R are highlighted.

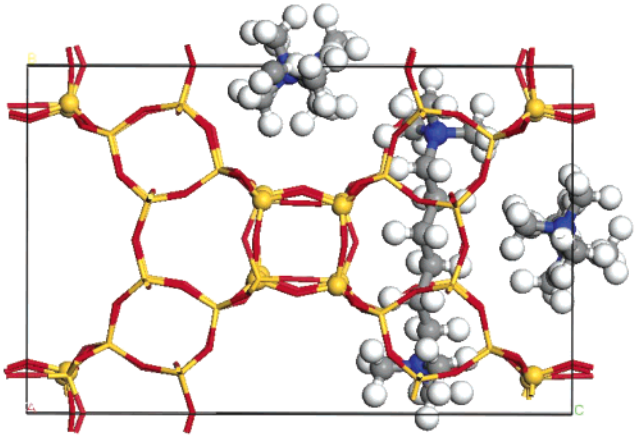

Figure 4. Structure of ITQ-24 with hexamethonium. T sites in D4R are highlighted.

TABLE 3: Energy of Interaction between Individual Hexamethonium Molecules and the Micropores in EU-1, ITQ-13, ITQ-22, and ITQ-24

	$E_{zeo'-SDA}$ (eV)			
zeolite	cavity	10 MR	12 MR	ΔE_{Fluor} (eV)[a]
EU-1	−1.58			
ITQ-13	−1.55			−0.60
ITQ-22		−1.58	−1.38	−0.59
ITQ-24		−1.60	−1.23	−0.53

[a] Electrostatic energy contribution corresponding to the inclusion of F^- anions. This energy corresponds to the sum of electrostatic interaction over the following terms: zeo′−SDA^+, zeo′−F^-, SDA^+−SDA^+, F^- −F^-, and SDA^+−F^-. This gives a comparative idea between the different structures on how the inclusion of fluorine may stabilize each structure. The F^- anions have been located inside D4R units, except in EU-1, where this has not been calculated because the location of F^- anions is not known. The F^- anion contents per unit cell are 4 F^- anions per 56 Si atoms, 4 F^- anions per 112 Si atoms, and 2 F^- anions per 56 Si atoms in ITQ-13, ITQ-22, and ITQ-24, respectively. Provided there is 1 D4R unit for every 28 Si atoms, this means that D4R units are fully occupied with F^- anions. In ITQ-13, two F^- anions have been located in $[4^15^26^2]$ cages.

further stabilization, because of the multidirectional type of interactions established. All these results point to the fact that structures formed by pores of less than 12 MR channels are favored when using the hexamethonium as an SDA.

The $E_{zeo'-SDA}$ term is dependent on the zeolite−SDA matching and the number of SDA molecules that can be hosts in the micropore structures with larger micropore volumes, which are usually higher in energy,[4,28] and admit larger loadings; this gives them the *opportunity* to be stabilized by reducing the global energy (E_{Total}) through favorable (more-negative) values of the $E_{zeo'-SDA}$ term. This would be the case for the least-dense and less-stable ITQ-24 structure ($E_{zeo'}$ = −128.54 eV/SiO_2 in Table 2), where the term $E_{zeo-SDA}$ = −0.066 eV/SiO_2 (see Table 2) is the lowest (most-favorable) energy for the zeolite structures studied here. However, the stabilization achieved by the zeolite−SDA interaction is not enough to compensate the higher values for the other energy terms and, therefore, the global energy (E_{Total}) is still higher than that for EU-1 and ITQ-13.

TABLE 4: Maximum Aluminum Content of Zeolites Corresponding to Complete Filling of the Corresponding Micropores with the SDA, $[Me_3N-(CH_2)_6-NMe_3]^{2+}$[a]

zeolite	$E_{zeo'}$ (eV/TO_2)	Al/(Si + Al)
ITQ-24	−128.54	0.096
ITQ-22	−128.56	0.072
ITQ-13	−128.58	0.072
EU-1	−128.58	0.072

[a] The energy ordering of the structures is relative and the values can be found in Table 2. ($E_{zeo'}$). The neutralization of one SDA^{2+} with 2 Al atoms allows one to establish that Al/(Si + Al) = 2[SDA]/SiO_2. This equation relates the Al content to the SDA concentration (in molecules/SiO_2).

5.2. Role of the Water/Silicon Ratio. As shown by previous studies,[5] the water/silicon ratio is important and is also used as a variable of synthesis that can be used to select through structures of different densities. Generally, the lower the water/silicon ratio, the lower the framework density of the zeolite phase that is formed. In the experiments, the denser phases EU-1 and ITQ-13 (see footnote "b" in Table 2) are obtained at higher dilution (entries 5, 6, and 11 in Table 1). On the other hand, ITQ-24, which is the least dense of the structures in this study, is always obtained at low water/silicon ratios (entries 7 and 12−14 in Table 1).

5.3. Role of Aluminum. Taking into account the micropore volume of the different structures, the maximum aluminum content that the structures can host is shown in Table 4. This data show that, at aluminum contents of 0.072−0.096, which approximately correspond to 9 < Si/Al < 13, zeolites EU-1 and ITQ-13 cannot be obtained and ITQ-24 should be the synthesis product (see entries 12−14 in Table 1). The experimental results (entries 2 and 7) in Table 1 (with Si/Al = 20) show that the synthesis product becomes ITQ-24 + EU-1, instead of ITQ-13. The discrepancy between the theoretical (Si/Al = 13) and experimental (Si/Al = 20) values of the Si/Al limit below which ITQ-13 (and EU-1) cannot be obtained show some discrepancy, even though we believe that the general trend can be reasonably explained. An additional experiment (entry 15 in Table 1) shows that, at Si/Al = 10, an amorphous phase is obtained, which also means that we are above the maximum amount of aluminum that ITQ24 can hold. This corresponds very closely to the value Si/Al = 9 that was reported previously.

5.4. Role of Germanium and Fluorine. The influence of fluorine and germanium has also been investigated. A common structural characteristic of some of these structures (ITQ-13, ITQ-22, and ITQ-24) is the presence of double four ring (D4R) units. These secondary building units are known to be favored if germanium is introduced in the synthesis gel.[29] This has an effect in the formation of the final structure, and, in principle, structures without D4Rs will not be formed. Previous studies also indicate that germanium contents of ~2−3 Ge atoms per D4R unit are the most favorable,[29] and these corresponds to 8.3 < Si/Ge < 13 for ITQ-13, ITQ-22, and ITQ-24, because all three structures have 8 T(D4R) units per 28 T(total) atoms, which is one D4R unit per 28 T atoms. At higher germanium contents, when more than three Ge atoms are present in each D4R unit (or some Ge appears in other positions), the relative stability of the zeolites may change if some structure can accommodate the subsequent distortions introduced by the additional Ge atom better than others. F^- anions act cooperatively with Ge in a further stabilization of not only D4R units but also other small cages present in the structure (such as $[4^15^26^2]$ in ITQ-13) and the synthesis is accelerated.[30] Thus, under synthesis conditions where EU-1 and ITQ-13 are competing, EU-1, which is a structure without D4R units, disappears from the synthesis products and ITQ-13 is formed when F^- anions are introduced in the gel, as can be observed in entries 3 and 4 of Table 1. An additional set of calculations has been performed including F^- anions inside each D4R unit of ITQ-13, ITQ-22, and ITQ-24, and the results are presented in Table 3. Although, as previously mentioned, all the structures have one D4R unit per 28 Si atoms, the ratio of F^- anions per hexamethonium molecule is not the same, because of the different porosity of each structure. A special case appears with ITQ-13, where the F^- anion is experimentally observed in half of the $[4^15^26^2]$ cages present in the structure.[30] When the amount of F^- anions included inside small cages is not enough to neutralize the positive charges of the SDA, the SDA is believed to be neutralized by forming hexamethonium fluoride. As in a previous work,[15] a neutralized SDA (whose nonzero atomic charges give an overall neutral molecule) has been chosen as an approximation to model the experimental situation. A smaller distance between the F^- anions and hexamethonium cations is expected to provide a larger electrostatic stabilization. Therefore, the electrostatic energy that corresponds to the interaction between the F^- anions and hexamethonium cations has been calculated, and the results (Table 3) indicate that ITQ-13 and ITQ-22 are favored, with respect to ITQ-24. In fact, the latter structure appears only at aluminum contents that cannot be reached by the other two. ITQ-24 does not appear by including fluorine in any of the entries in Table 1, whereas the presence of fluorine is associated with the appearance of an ITQ-22 phase (entry 3 in Table 1) or an ITQ-13 phase (entries 4, 5, and 10 in Table 1).

Ge atoms are known to influence the chemistry of the nucleation processes, and this may have an effect on the final structure that is synthesized. The main reason ITQ-13, ITQ-22, and ITQ-24 are obtained in the experiments of Table 1 is because of the introduction of germanium, and none of them are found under those conditions if germanium is not present in the synthesis gel. Although this study does not focus on how the zeolite nucleates around the hexamethonium cations, it is clear that Ge atoms provide different stabilities to the different zeolite frameworks and this changes the final stability. Because the previous results in Table 2 correspond to calculations with pure silica crystals, we have now introduced germanium in the structures to study whether this affects the relative stability of the zeolites, and the results are summarized in Table 5. A Si/Ge ratio of 13 has been chosen, and for this ratio, the Ge atom is believed to be located in the D4R position;[29] this means that two Ge atoms per D4R unit are present, at opposite corners, in the zeolites ITQ-13, ITQ-22, and ITQ-24, at low germanium concentrations. In EU-1, where the Ge atom location is not known, we have selected the lowest-energy configuration out of a random sampling of 100 possibilities generated by a simple algorithm, as in a previous study.[31] The results (Table 5) show that, while the hexamethonium energy and the zeo′−SDA energy are very similar for pure silica and germanium-containing entries, differences in the global energy (E_{Total}) are observed. These are mainly due to changes in the zeolite energy that are due to the incorporation of germanium. Although the relative order of increasing energy between ITQ-13, ITQ-22, ITQ-24 is maintained upon Ge substitution ($E_{zeo'}$ in Tables 2 and 4), EU-1 shows a destabilization—its global energy is higher than that of the other three structures when germanium is introduced. This observation shows that increasing the germanium content favors ITQ-13 and ITQ-22 (entries 8 and 9 in Table 1), with respect to the EU-1 structure (entries 1 and 3 in Table 1), and ITQ-24 (entry 14 in Table 1) also becomes more favorable than EU-1 (entry 7 in Table 1).

TABLE 5: Energetic Contributions and Total Energy (as from eq 1) to the Synthesis of EU-1, ITQ-13, ITQ-22, and ITQ-24 When Hexamethonium Dihydroxide is Used as a Structure Directing Agent (SDA) and the Zeolite Has a Si/Ge Ratio of 13[a]

zeolite	$E_{zeo'}$ (eV/TO_2)[b]	ΔE_{SDA} (eV)[c]	$\Delta E_{zeo'-SDA}$ (eV/TO_2)[c]	ΔE_{Total} (eV/TO_2)
EU-1	−128.21	0.013	−0.054	−128.26
ITQ-13[d]	−128.25	0.022	−0.054	−128.30
ITQ-22[d]	−128.23	0.017	−0.051	−128.29
ITQ-24[d]	−128.22	0.019	−0.061	−128.28

[a] All other variables are as given in Table 2. F^- anions have not been included in the calculations. [b] Framework energy of unloaded zeolites per TO_2 unit (first term in eq 1). This corresponds to the zeolite geometry as with the SDA optimized inside. The corresponding number of SiO_2 units are 112 for EU-1, ITQ-22, and ITQ-24, and 56 for ITQ-13. [c] As given in Table 2. [d] There is 1 D4R unit per 28 Si atoms in ITQ-13, ITQ-22, and ITQ-24, of which the two opposite corners are occupied by Ge atoms.

6. Conclusions

Four zeolite structures—EU-1, ITQ-13, ITQ-22, and ITQ-24—have been found in the synthesis with germanium in the synthesis gel. Germanium is known to favor structures that contain D4R (such as ITQ-13, ITQ-22, and ITQ-24), and the selectivity between them is explained by decomposing the energy in three contributions: the zeolite structural stability, the zeolite−structure directing agent (SDA) interactions, and the SDA strain as occluded in the micropore. The relatively low match between the SDA used (hexamethonium dihydroxide) and the zeolite structures is the reason none of these structures are favored over the others, in regard to the zeolite−hexamethonium interactions; therefore, synthesis factors should be considered to be responsible for directing the synthesis toward one structure or another. We have found that other factors are important, in regard to the global energy of the zeolites, including the aluminum content, the water/silicon ratio, and the presence of Ge atoms or F^- anions. The aluminum content becomes important at low Si/Al ratios, where the most-porous structure ITQ-24 is favored. Also, ITQ-24, which is the least-dense structure, is favored at low water/silicon ratios. The presence of germanium allows one to eliminate EU-1 (at

sufficiently high germanium content) from the synthesis products and possibly favors ITQ-22 at low Si/Ge ratios. The F^- anions have a tendency to disfavor ITQ-24 from the synthesis products. The combination of all these factors, which can be understood from the energetic viewpoint, allows the synthesis to be driven toward each particular structure.

In other words, we have seen that theoretical calculations where the different energy-contributing terms are individualized clearly help to rationalize the influence of the different synthesis variables on the relative synthesis probability of various competing structures. This becomes especially interesting when less-rigid/less-selective organic SDA agents are used. In those cases, it is shown that, by rationally combining the number of framework charges generated (the T^{III} concentration), selection of the silica mobilizing agent (OH^- or F^-), and the introduction of another T^{IV} atom (Ge), can help to predict the optimum synthesis conditions to select one or another of the competing structures. We are aware that this is still an initial small step toward zeolite synthesis by design and recognize that much more work that combines theory and experiments will be required.

Acknowledgment. We thank Generalitat Valenciana for providing funds through the project GV01-492. We also thank Centro de Cálculo de la Universidad Politécnica de Valencia for the use of their computational facilities.

References and Notes

(1) Davis, M. E.; Lobo, R. F. *Chem. Mater.* **1992**, *4*, 756.
(2) Baerlocher, Ch.; Meier, W. M.; Olson, D. H. *Atlas of Zeolite Framework Types*, 5th ed.; Elsevier: Amsterdam, 2001. (Available via the Internet at http://www.iza-structure.org.)
(3) Lawton, S. L.; Rohrbaugh, W. J. *Science* **1990**, *247*, 1319.
(4) Yang, S.; Navrotsky, A. *Microporous Mesoporous Mater.* **2002**, *52*, 93.
(5) Barrett, P. A.; Boix, E. T.; Camblor, M. A.; Corma, A.; Diaz-Cabañas, M. J.; Valencia, S.; Villaescusa, L. A. *Proceedings of the 12th International Zeolite Conference*; Treacy, M. M. J., Marcus, B., Higgins, J. B., Bisher, M. E., Eds.; Materials Research Society: Pittsburgh, PA, 1998; p 1495.
(6) Corma, A.; Diaz-Cabañas, M. J.; Martinez-Triguero, J.; Rey, F.; Rius, J. *Nature* **2002**, *418*, 514.
(7) Corma, A.; Rey, F.; Valencia, S.; Jorda, J. L.; Rius, J. *Nature Mater.* **2003**, 493.
(8) Davis, M. E.; Zones, S. I. In *Synthesis of Porous Materials: Zeolites, Clays and Nanostructures*; Occelli, M. L., Kessler, H., Eds.; Marcel Dekker: New York, 1996; p 1.
(9) Castañeda, R.; Corma, A.; Fornes, V.; Rey, F.; Rius, J. *J. Am. Chem. Soc.* **2003**, *125*, 7820.
(10) Lobo, R. F.; Zones, S. I.; Davis, M. E. *J. Inclusion Phenom. Mol. Recognit. Chem.* **1995**, *21*, 47.
(11) Corma, A.; Diaz-Cabañas, M. J.; Fornes, V. *Angew. Chem., Int. Ed.* **2000**, *39*, 2346.
(12) Gittleman, C. S.; Bell, A. T.; Radke, C. J. *Catal. Lett.* **1996**, *38*, 1.
(13) Zones, S. I.; Hwang, S.-J. *Microporous Mesoporous Mater.* **2003**, *58*, 263.
(14) Harris, T. V.; Zones, S. I. *Stud. Surf. Sci. Catal.* **1994**, *84*, 29.
(15) Sastre, G.; Leiva, S.; Sabater, M. J.; Gimenez, I.; Rey, F.; Valencia, S.; Corma, A. *J. Phys. Chem. B* **2003**, *107*, 5432.
(16) Gale, J. D. *J. Chem. Soc., Faraday Trans.* **1997**, *93*, 629.
(17) Sanders, M. J.; Leslie, M.; Catlow, C. R. A. *J. Chem. Soc., Chem. Commun.* **1984**, 1271.
(18) Jackson, R. A.; Catlow, C. R. A. *Mol. Simul.* **1988**, *1*, 207.
(19) Lewis, D. W.; Freeman, C. F.; Catlow, C. R. A. *J. Phys. Chem. B* **1995**, *99*, 11194.
(20) Lewis, D. W.; Catlow, C. R. A.; Thomas, J. M. *Chem. Mater.* **1996**, *8*, 1112.
(21) Catlow, C. R. A., Ed. *Modelling of Structure and Reactivity in Zeolites*; Academic Press: London, 1992.
(22) Catlow, C. R. A.; Bell, R. G.; Gale, J. D. *J. Mater. Chem.* **1994**, *4*, 781.
(23) Kiselev, A. V.; Lopatkin, A. A.; Shulga, A. A. *Zeolites* **1985**, *5*, 261.
(24) Oie, T.; Maggiora, T. M.; Christoffersen, R. E.; Duchamp, D. J. *Int. J. Quantum Chem., Quantum Biol. Symp.* **1981**, *8*, 1.
(25) George, A.; Catlow, C. R. A. *Zeolites* **1997**, *18*, 67.
(26) Sastre, G.; Lewis, D. W.; Catlow, C. R. A. *J. Phys. Chem.* **1996**, *100*, 6722.
(27) Sastre, G.; Lewis, D. W.; Catlow, C. R. A. *J. Phys. Chem. B* **1997**, *101*, 4575.
(28) Henson, N. J.; Cheetham, A. K.; Gale, J. D. *Chem. Mater.* **1994**, *6*, 1647.
(29) Sastre, G.; Vidal-Moya, J. A.; Blasco, T.; Rius, J.; Jorda, J. L.; Navarro, M. T.; Rey, F.; Corma, A. *Angew. Chem., Int. Ed.* **2002**, *41*, 4722.
(30) Vidal-Moya, J. A.; Blasco, T.; Rey, F.; Corma, A.; Puche, M. *Chem. Mater.* **2003**, *15*, 3961.
(31) Sastre, G.; Fornes, V.; Corma, A. *J. Phys. Chem. B* **2002**, *106*, 701.